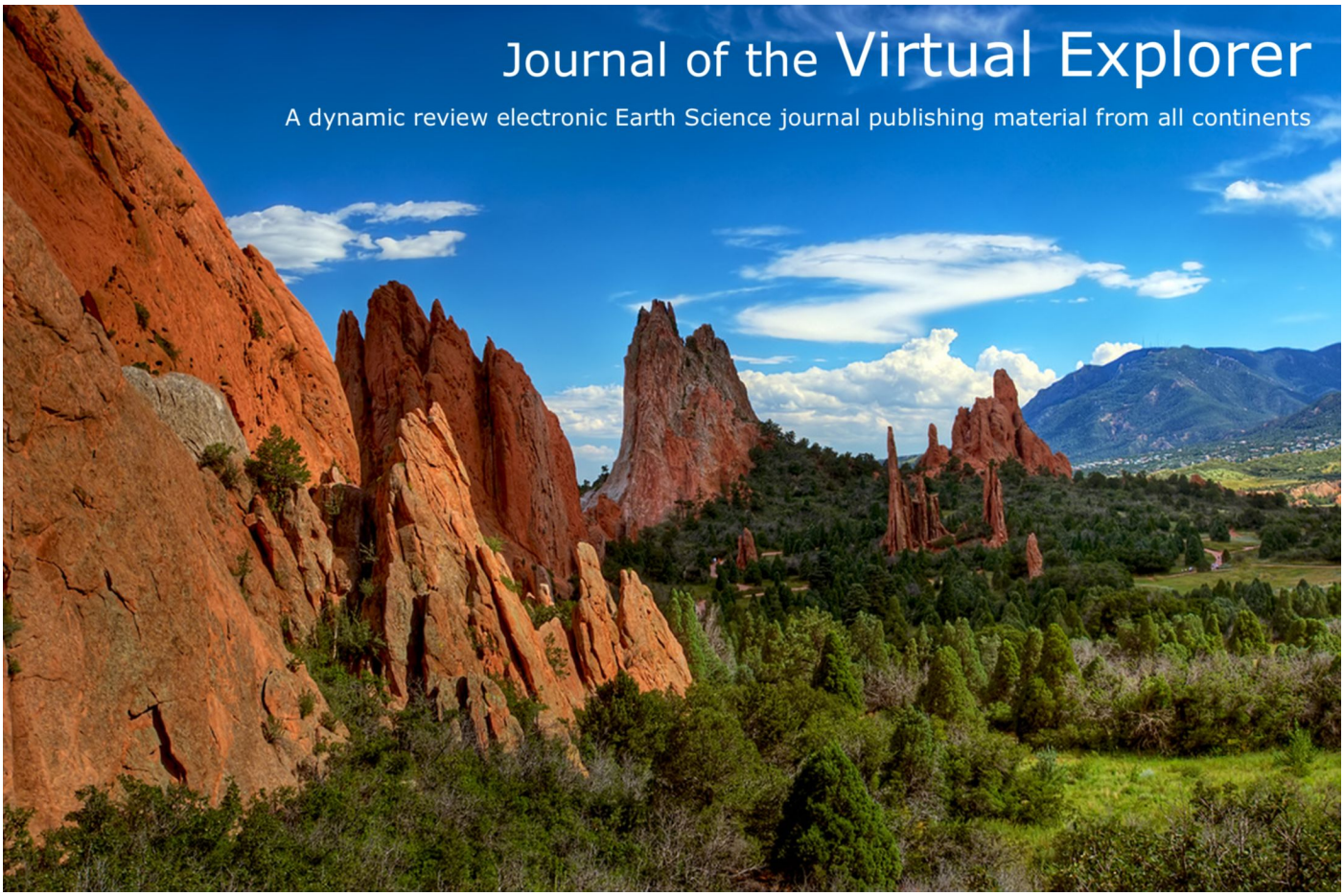

Mineralogical evidence for magma mingling in the Plio-Quaternary volcanic rocks (Central Iran)

Shahrzad Sherafat, Iraj Noorbehesht, Mahmoud Khalili

Journal of the Virtual Explorer, Electronic Edition, ISSN 1441-8142, volume **31**, paper 1
In: (Eds.) Guiting Hou and Gideon Rosenbaum, General Contributions, 2009.

Mineralogical evidence for magma mingling in the Plio-Quaternary volcanic rocks (Central Iran)

Shahrzad Sherafat, Iraj Noorbehesht, Mahmoud Khalili

Journal of the Virtual Explorer, Electronic Edition, ISSN 1441-8142, volume **31**, paper 1
In: (Eds.) Guiting Hou and Gideon Rosenbaum, General Contributions, 2009.

Abstract: The Plio-Quaternary calc-alkaline dacitic and rhyodacitic lava flows and domes are located in Yazd province within the central Iranian magmatic belt. These rocks are composed of plagioclase, hornblende, biotite, and quartz set in a glassy to felsity groundmass. The subrounded to vesicular magmatic enclaves, ranging in size from a few millimeters to a few centimeters and similar mineral assemblage to their host rocks, are recognized in the studied rocks.

The variety of disequilibrium features which are observed in all phases can be taken as an evidence of magma mingling. The plagioclase phenocrysts exhibit sieved- and normal-type populations, dusty core or rim, a wide range in rim compositions and oscillatory zoning. Hornblende and biotite phenocrysts have reaction rims and are replaced by Fe-Ti oxides indicating disequilibrium crystallization with magma. Both hornblende and biotite crystals show reverse zoning and the Mg/Mg +Fe ratio increases from core to rim. Quartz phenocrysts are corroded and embayed.

Although the existence of sieve texture in plagioclase and reaction rims on mafic minerals may be considered to be the result of decompression, this cannot explain the observed compositional changes and the co-existence of normal types of plagioclase in the same sample. In fact, other evidence such as resorbed and embayed phenocrysts indicate that the mafic magma is intruded into felsic magma and magma mingling was a viable process in the generation of these volcanics.

Citation: Sherafat, S., Noorbehesht, I., Khalili, M. 2009. Mineralogical evidence for magma mingling in the Plio-Quaternary volcanic rocks (Central Iran). In: (Eds.) Guiting Hou and Gideon Rosenbaum, *Journal of the Virtual Explorer*, volume **31**, paper 1, doi: 10.3809/jvirtex.2009.00214

Introduction

Magma mixing or mingling is one of the significant processes in the evolution of magmas. The term mixing (Sparks and Marshal, 1986) is applied when the magmas have a homogeneous composition, whereas the term mingling is used if the magmas are mixed physically but heterogeneously, with banding or enclaves/inclusions present.

In the mixed magmas, the compositions and temperatures of the end-member magmas can be determined from the compositional and textural features of phenocrysts (Wallace and Carmichael, 1994). However, in the petrological literatures, magma mixing or mingling is the most common process for the origin of intermediate volcanic rocks.

Petrology and mineral chemistry of the Plio-Quaternary volcanic rocks within this part of Iran have been little studied. Although, there are a number of studies on the Jurassic Shir-Kuh batholith (i,e Khalili, 1997) and the Oligo-Miocene granitoids associated with porphyry copper deposits in the study area (Zarrasvandi, 2005), the study of Plio-Quaternary subvolcanic rocks is generally overlooked.

The research area lies in Central Iran and located in west and southwest of Yazd province. Based on subdivision of Iran, this area belongs to Central Iranian Magmatic Belt (Stocklin, J., 1968) known as Urumieh-Dokhtar Volcanic Belt (UDVB). This zone trending northwest-southeast, is parallel to the Zagros fold-and-thrust belt (Fig.1). Magmatic activity in the UDVB from Eocene to Quaternary age represents an Andean type magmatic arc (Takin, 1972; Sengör, 1990; Alavi, 1994) that peaked during the Eocene. Plio-Quaternary volcanic rocks that studied in this paper, consist of several domes and lava flows. Surk and Ernan mountains are the northern and southern part of this area, respectively. Other bodies are located between them in Shamsabad, Aliabad, Abdollah, Ostaj and Bouragh regions.

The purpose of this paper is to describe the petrography, mineral-chemistry and geochemistry of the Plio-Quaternary rocks of this part of UDMA as well as discussing the petrogenesis of these rocks.

Figure 1. Location map showing three main tectonic zones of Iran

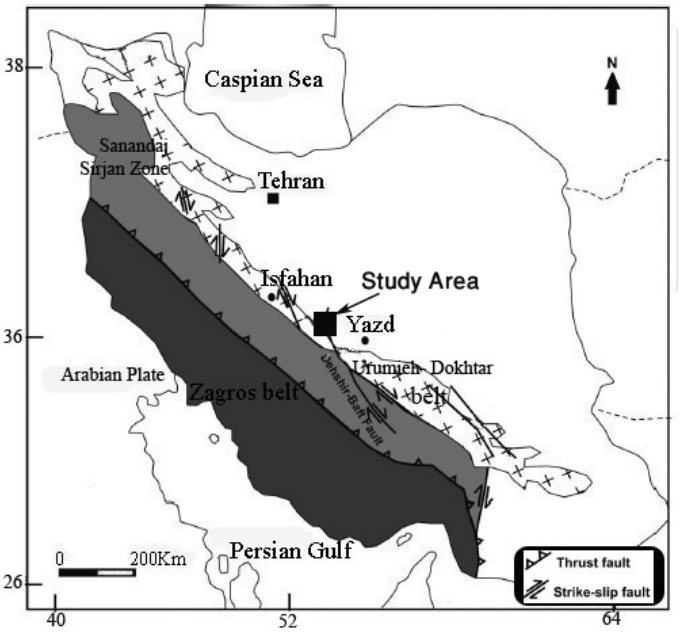

Geological setting

The oldest rocks in the study area (Fig.2) are the dolomite, sandstone and limestone of the Triassic period which are exposed in the north parts of the region. These rocks are followed by the formations given below:

1. The Sangestan formation. This formation is composed of a very thick sequence of red sandstone and conglomerate. The Shir-Kuh batholith is overlain unconformably by this formation (Khosrotehrani and Vazirimoghadam, 1993).

2. The Taft Formation. The Taft Formation consists of massive to bedded dark grey marine carbonates (Khosrotehrani and Vazirimoghadam, 1993). These rocks were probably deposited on a continental shelf. A Barremian-Lower Albian age was reported for this formation.

3. The Eocene association. The Eocene conglomerate and volcano-sedimentary rocks overlain the Mesozoic sedimentary sequences. Andesitic lavas, trachyandesite and pyroclastic rocks are the main products of Eocene volcanic activity.

4. The Oligocene-Miocene-Pliocene rocks. The Oligo-Miocene plutons consist of granite, granodiorite, tonalite, quartzmonzodiorite and diorite (exposed in the west and northwest of the study region) that intrude into the Mesozoic and Paleocene units (Zarasvandi *et al.*, 2004). The Neogene dacitic and rhyodacitic domes and flows are the

youngest magmatic activity in this region. These volcanic rocks crop out in the north (Surk, Kuhe-Mile), central (ShamsAbad, Ostaj, Abdollah, G-Ali Abad) and southern (Buragh, Darreh Zereshk, Turan Posht, Ernan) parts of the study area. Rhyodacitic and dacitic flows display flow banding, autobrecciated upper carapaces and columnar jointing. They have numerous sub-rounded, vesicular enclaves of varying size (few millimeters to few centimeters) with granular and fine-grained textures.

5. The youngest rocks in these regions are the Quaternary deposits large tabular and dome like travertine deposits (Hajmolaali and Alavi, 1993) generated by geothermal activity. The Dehshir-Baft dextral strike-slip fault and related faults are the major structural features that seperate the Mesozoic Formations (Cretaceous limestone) from the Cenozoic Formation (Eocene andesite and tuffs).

Methodology

Electron microprobe mineral analyses

Composition of plagioclase, amphibole and biotite phenocrysts in volcanic rocks were analyzed by wavelength dispersive spectrometry, using a Cameca SX50 electron microprobe (EMPA) at the University of Oklahoma, Norman (USA). Probe conditions were 20 kV accelerating voltage, 20 ηA beam current, a spot size of 3 µm, and measurement times of 30 s per peak for all elements. Analyses were calibrated against appreciate standards before each session. Minimum level of detection (at 3-sigma above mean background) of </= 0.20 wt% of the oxide for all components exept Ba (0.09 wt% BaO), F (0.10 wt%) and Sr (0.03 wt% SrO).

The data for amphibole was then recalculated for Fe^{+3} using Droop's (1987) equation. Amphibole, biotite and plagioclase are analyzed as part of this study. Representative analyses are given in Table 1.

Whole rock geochemistry

Samples for geochemical analysis were prepared by crushing in an agat disk mill. Half gram sample leached with 3 milliliter HCl-HNO_3-H_2O at 95 °C for one hour, diluted to ten milliliter and then analysed by Inductively Coupled Plasma Mass Spectrometer (ICP-MS) for major and trace elements at the ACME analytical laboratories (Vancouver, Canada). Replicate analysis of International Standards indicate accuracy to within 5-10 relative percent of standard values for major and minor elements.

Figure 2. Simplified geological map

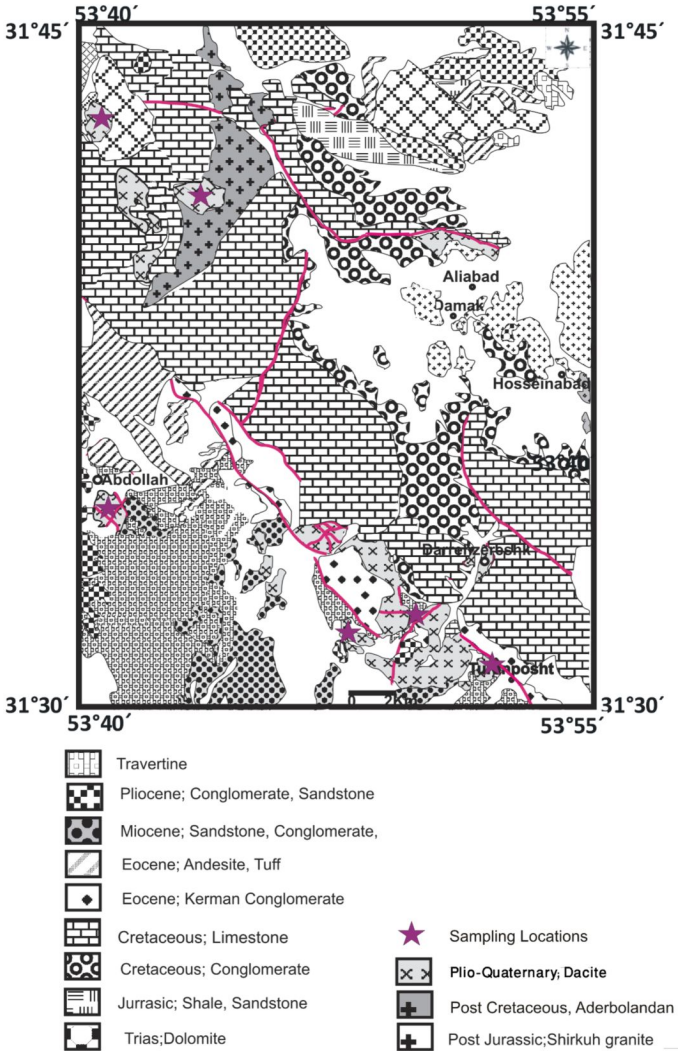

Simplified geological map of the study area (after Hajmolaali and Alavi, 1993)

Petrography

The phenocryst assemblages of dacite and rhyodacite consist of plagioclase-hornblende-biotite-quartz and locally sanidine set in a glassy to felsity matrix. The predominant textures are microlity porphyry, hyalomicrolity porphyry, glomeroporphyry and felsity.

The plagioclase phenocrysts often show normal or oscillatory zoning. Two types of plagioclases are found together. The first type is quite clear and characterized by normal zoning. The second type is marked by sieve or dusty texture in the core or rim (Fig. 3a, 3b).

Hornblende and biotite are partially to completely oxidized forming opacite pseudomorphs (Fig. 3c) and replacing by Fe-Ti oxides or having a reaction rims indicating disequilibrium crystallization.

Euhedral to subhedral phenocrysts of quartrz are strongly resorbed (rounded grains). Some quartz grains are embayed and corroded (Fig. 3d).

Zircon and apatite are present as inclusions in biotite and amphibole.

The matrix is typically glassy (colorless, variably devitrified), locally flow banded with fine-grain plagioclase crystallites. Devitrification of matrix glasses generated fesitic matrix.

Numerous sub-rounded enclaves are common in dacitic and rhyodacitic rocks. These enclaves with fine grain and granular-texture are similar in mineral assemblage to their host rocks (Fig. 3e).

Figure 3. Disequilibrium textures in rhyodacites and dacites

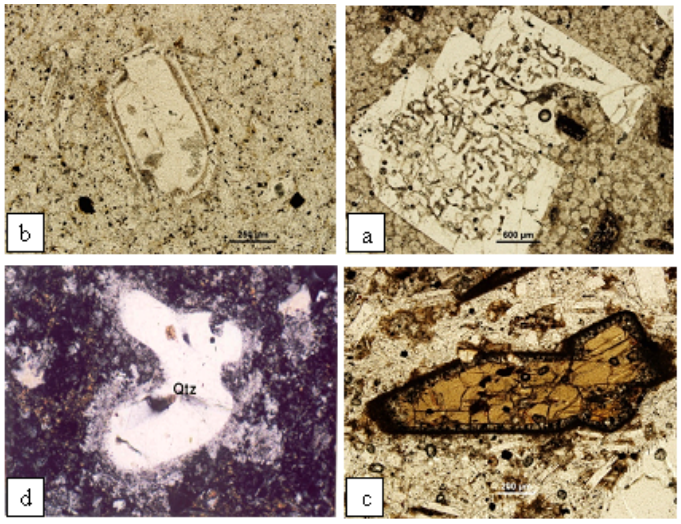

Photomicrograph of disequilibrium textures in rhyodacites and dacites, all photographs were given in plan polarizad light. (a)Sieved texture of plagioclase crystals; (b) dusty rim in plagioclase; (c) development of reaction rims in amphibole; (d) embayed and corroded quartz; (e) find-grain and grandular-tecture rounded enclave.

Mineral chemistry

Plagioclase

The plagioclase phenocrysts up to 25% modal are the most abundant mineral in the dacite and rhyodacitic rocks. Microlithic plagioclases are found in glassy or felsitic matrix. The plagioclase phenocrysts are typically zoned and show euhedral to subhedral shapes. Compositional determination shows that the plagioclase crystals in these rocks are oligoclase to andesine in core (An_{20} to $An_{44.7}$) and andesine in rim ($An_{23.1}$ to $An_{40.4}$).

Two types of plagioclases are observed in studied rocks. The first type is clear having normal zoning.

The second type indicates resorption textures such as sieved texture (with a clear core and a sieved rim, or vice versa), dusty core or rim and reverse zoning. In these minerals, the observed maximum compositional range from core to rim is 13.2 mole %An. Moreover, the zoning is abrupt (Table 1). Sieved texture in plagioclase phenocrysts is described as the interconnected inclusions of glass or other matrix materials (Shelly, 1993). It also formed by decompression when magma rises towards the surface (Nelson and Montana, 1992). According to Stamatelopoulou-Seymour, *et al.* (1990), if sieved plagioclases were formed due to mixing, a calcic sieve-texture core should be followed by a resorption surface associated with a sudden change in An content of at least 10%. The heterogeneity of plagioclase rims within a single sample indicate a complex origin and may be due to magma mixing event (Wallace and Carmichael, 1994).

In dusty plagioclases, groundmass glass is sometimes detected in the dusty rim of plagioclase. The maximum An% in the dusty rim is about 46% whereas it is approximately 26% in the clear part. Several lines of evidence such as the corrosion of plagioclases, the variations in compositional zoning, the sieved texture and the dusty rims suggest that precipitation of plagioclase crystals are inconsistent with physico-chemical conditions of magma (Tsuchiyama, 1985; Stamatelpoulou-Seymour, *et al.* 1990)

Table 1. Representative plagioclase analyses from Plio-Quaternary volcanic rocks (C: Core; C/R: Core to Rim; R: Rim; VR: Very Rim; Cations per 8 oxygens)

	Surk		**Bour-agh**			**Ernan**					**S-Ern-an**	
Sam-ple	C3-C	C3-R	BU-C	BU-C/R	BU-R	ER1-C	ER1-R	ER2-C	ER2-C/R	ER2-R	SE-C	SE-R
SiO_2	59.99	57.11	57.24	55.05	59.5	62.93	58.58	58.68	57.87	60.26	63.15	61.05
TiO_2	0.01	0.02	0	0.02	0	0.01	0	0	0.01	0	0	0
Al_2O_3	24.5	26.89	26.96	28.23	25.5	23.28	25.57	26.08	26.93	24.65	23.56	25.12
Fe_2O_3	0.19	0.3	0.21	0.17	0.2	0.06	0.15	0.15	0.19	0.15	0.11	0.17
MnO	0	0	0	0	0	0	0.01	0	0	0	0.01	0.001
MgO	0.01	0.02	0	0.01	0	0	0	0	0.01	0	0	0.01
CaO	5.92	8.66	8.31	10.02	6.7	4.25	7.04	7.4	8.14	5.93	4.5	6.3
Na_2O	7.79	6.56	6.85	5.67	7.69	8.77	7.49	7.36	6.86	8.11	9.08	8.12
K_2O	0.86	0.51	0.24	0.2	0.38	0.93	0.47	0.29	0.28	0.58	0.54	0.34
Total	99.72	100.3	100.07	99.56	100.12	100.32	99.5	100.21	100.47	99.91	101.18	101.41
An%	28.1	41	39.6	48.8	31.8	20	33.3	35.1	39	27.8	20.9	29.4
	Ostaj		**G-Alia-bad**								**Abdol-lah**	
Sam-ple	Os1-C	Os1-R	Ga1-C	Ga1-R	Ga2-C	Ga2-R	Ga2-VR	Ga3-C	Ga3-C/R	Ga3-R	Ab-C	Ab-R
SiO_2	60.42	62.73	49.29	61.41	53.5	53.94	57.36	60.56	55.89	62.24	58.58	59.74
TiO_2	0	0	0	0.04	0	0.01	0.03	0	0	0.08	0.01	0.01
Al_2O_3	24.52	23	31.56	23.48	28.85	28.38	26.11	24.29	27.17	23.41	25.88	24.88
Fe_2O_3	0.12	0.14	0.47	0.41	0.16	0.44	0.49	0.14	0.15	0.45	0.18	0.19
MnO	0.01	0.01	0.01	0.01	0	0.01	0.03	0.02	0	0.02	0	0.01
MgO	0	0	0.02	0.02	0	0.03	0.04	0.01	0	0.01	0.01	0.01
CaO	5.63	3.97	13.91	4.76	10.8	10.49	7.98	5.56	8.92	4.41	7.42	6.4
Na_2O	8.05	8.89	3.5	8.73	5.24	5.59	6.89	8.17	6.5	8.9	7.27	7.61
K_2O	0.55	0.83	0.09	0.65	0.17	0.2	0.35	0.52	0.27	0.71	0.3	0.47
Total	99.61	99.64	99.15	99.82	99.17	99.42	99.57	99.56	99.2	100.63	99.78	99.46
An%	27	18.8	68.3	22.3	52.7	50.4	38.3	26.5	42.5	20.6	35.4	30.9

Amphibole

Based on the classifications of Leake (1978), amphiboles from dacite and rhyodacites fall in the calcic amphibole field (except for opacitized rims which classified as Mg-Fe-Mn-Li amphiboles). The amphiboles from different regions display different composition. Those from Surk, Shamsabad, Ostaj and Abdollah regions vary from tschermakite to magnesio-hornblende, whereas the ones from Ernan and S-Ernan are mainly magnesio-hastingsite (Table 2).

The amphiboles in particular, those from Surk, Ernan and S-Ernan show normal or reverse zoning. The Mg-number in reverse zoning amphibols is increased from core to rim. These minerals occasionally have reaction rims partially to completely oxidized forming "opacite" pseudocmorphs caused by replacing of amphiboles with Fe-Ti oxides.

If the water content of the magma is too low for amphibole stability, reaction rims are developed (Rutherford and Hill, 1993; Feeley and Sharp, 1996). Thus, amphiboles in the studied rocks display disequilibrium characteristics such as reverse zoning, reaction rims and pseudomorphs after hornblende.

Biotite

Several features particularly the existence of oscillatory and reverse zoning (Mg-number of the biotite increase from core to rim, Table 3), the reaction rims and Fe-Ti oxide pseudomorphs after biotite, document that the biotite in the studied volcanic rocks is in a disequilibrium phase.

Table 2. Representative amphibole analyses from Plio-Quaternary volcanic rocks (C: Core; C/R: Core to Rim; R: Rim; VR: Very Rim; Cations per 22 oxygens; Tsch: Tschermakite; Cum: Cummingtonite; MgHb: Magnesiohornblende; MgHs: Magnesiohastingsite; Edn: Edenite)

		Surk		**Sham-sabad**		**Ernan**		**S-Ern-an**			**Abdol-lah**	
Sam-ple	C3-C	C3-C/R	C3-R	Sh-C	Sh-R	ER-C	ER-R	SE-C	SE-R	SE-VR	Ab-C	Ab-R
SiO_2	42.85	43.14	54.41	43.8	43.54	41.76	42.29	43.74	46.51	46.8	45.29	45.47
TiO_2	1.95	2.29	0.22	1.39	1.72	2.36	1.17	1.11	0.87	0.99	1.77	1.52
Al_2O_3	11.72	11.25	1.73	11.16	11.61	11.75	11.03	9.69	8.17	8.07	11.05	120.55
Fe_2O_3	15.32	14.14	18.55	7.98	8.43	13.09	18.24	19.07	15.53	14.94	9.89	10.15
MnO	0.21	0.21	0.58	0.1	0.08	0.1	0.3	0.53	0.46	0.38	0.08	0.12
MgO	12.51	13.51	24.76	15.43	14.71	13.01	11.53	10.39	12.89	13.54	12.25	15.2
CaO	10.66	10.44	1.11	9.75	10.01	10.99	10.72	10.95	10.89	10.99	11.25	10.95
Na_2O	2.16	2.18	0.12	2.15	2.3	2.44	2.43	1.74	1.65	1.65	2.05	2.18
K_2O	0.82	0.81	0.02	0.43	0.46	0.55	0.71	0.84	0.5	0.42	0.41	0.39
Total	98.4	98.05	101.6	92.51	93.16	96.44	99.65	98.33	97.67	98.05	97.17	96.78
Mg#	59.3	63	70.4	77.5	75.7	63.9	53	49.3	59.7	61.8	73.3	72.7
Name	Tsch	Tsch	Cum	Tsch	Tsch	MgHs	MgHs	Tsch	MgHb	MgHb	Tsch	MgHs
	Ostaj		**G-Alia-bad**									

		Surk		**Sham-sabad**		**Ernan**		**S-Ern-an**			**Abdol-lah**	
Sam-ple	Os-C	Os-R	Ga1-C	Ga1-R	Ga2-C	Ga2-C/R	Ga2-R	Ga3-C	Ga3-R	Ga4-C	Ga4-C/R	Ga4-R
SiO_2	42.22	44.9	41.42	40.57	39.66	40.87	40.21	46.04	47.72	39.6	40.79	40.66
TiO_2	2.77	1.38	1.64	1.99	2.17	1.56	1.83	1.1	0.96	1.9	1.88	1.67
Al_2O_3	12.02	8.86	13.05	13.75	14.09	13.95	13.86	8.58	6.86	14.02	14.09	14.06
Fe_2O_3	12.03	15.61	12.21	13.25	15.27	12.54	14.12	15.08	13.61	13.33	12.88	11.56
MnO	0.12	0.51	0.2	0.15	0.26	0.13	0.23	0.47	0.48	0.17	0.16	0.11
MgO	13.94	12.92	13.88	13.01	11.6	13.67	12.56	13.43	14.74	12.48	13.19	13.93
CaO	10.55	11.09	11.72	11.7	11.69	11.81	11.64	11.2	11.04	11.77	11.72	11.71
Na_2O	2.56	1.7	2.54	2.61	2.66	2.67	2.8	1.59	1.49	2.66	2.6	2.71
K_2O	0.56	0.74	0.44	0.48	0.65	0.47	0.57	0.45	0.37	0.56	0.49	0.58
Total	97.47	98.14	97.15	97.72	98.27	97.89	98.47	98.07	97.47	96.75	98.04	97.25
Mg#	67.4	59.6	67	63.6	57.5	66	61.3	61.4	65.9	62.5	64.6	68.2
Name	Tsch	MgHb	MgHs	MgHs	MgHs	MgHs	MgHs	Edn	MgHb	MgHs	MgHs	MgHs

Table 3. Representative biotite analysis from Plio-Quaternary volcanic rocks (C: Core; C/R: Core to Rim; R: Rim; VR: Very Rim)

	Surk			**Shamsa-bad**		**S-Ernan**			**Abdol-lah**	
Sample	C3-C	C3-R	C3-VR	Sh-C	Sh-R	SE-C	SE-C/R	SE-R	Ab-C	Ab-R
SiO_2	36.71	36.55	36.75	37.05	36.89	37.48	36.49	37.06	36.96	37.27
TiO_2	4.35	4.29	4.62	3.16	3.3	3.75	3.54	3.45	3.08	3.12
Al_2O_3	15	14.87	14.67	15.66	15.82	14.94	14.26	14.55	15.46	15.49
Fe_2O_3	14.34	15.09	13.71	16.41	17.59	17.5	21.51	19.15	14.5	13.93
MnO	0.09	0.09	0.08	0.09	0.2	0.18	0.29	0.22	0.1	0.1
MgO	15.84	15	16.15	14.05	13.58	13.29	10.87	12.41	14.96	15.49
CaO	0.01	0.02	0.03	0.08	0.03	0	0.01	0	0.05	0.02
Na_2O	0.59	0.72	0.7	0.55	0.48	0.56	0.29	0.34	0.26	0.47
K_2O	8.63	8.52	8.61	7.87	8.6	8.38	8.84	8.87	8.95	9.07
Total	97.59	96.93	97.38	95.84	97.39	96.9	97.19	96.96	95.77	96.82
Mg#	66.3	63.9	67.7	60.4	57.9	57.5	47.4	53.6	64.8	66.5
	S-Ernan			**G-Alia-bad**		**Ostaj**				
Sample	SE-C	SE-C/R	SE-R	Ga2-C	Ga2-R	Os-C	Os-R			

	Surk			**Shamsa-bad**		**S-Ernan**			**Abdol-lah**	
SiO_2	37.06	35.94	37.68	37.86	37.42	35.21	35.49			
TiO_2	3.42	3.41	3.41	3.76	3.87	3.8	3.85			
Al_2O_3	14.63	13.49	14.7	14.52	14.7	13.82	14.2			
Fe_2O_3	17.37	16.16	18.29	11.71	13.15	17.13	17.19			
MnO	0.22	0.11	0.19	0.13	0.19	0.2	0.22			
MgO	13.72	14.62	13.36	17.62	16.86	13.37	14.3			
CaO	0.01	0.5	0.06	0.01	0.15	0.42	0.37			
Na_2O	0.53	0.31	0.64	1.13	0.93	0.29	0.27			
K_2O	8.59	5.08	8.25	7.7	7.13	6.26	6.03			
Total	96.46	90.17	97.41	95.32	95.4	91.43	92.74			
Mg#	58.5	61.7	56.6	72.8	69.6	91.43	92.74			

Geochemistry

The concentrations of major elements of the studied rocks are presented in Table 4. Based on both (Na_2O + K_2O) vs SiO_2 (Le Bas *et al.*, 1986) and R1-R2 diagrams (De La Roche *et al.*, 1980) all the samples are classified as rhyolites, rhyodacite, dacites and rarely andesite (Fig. 4a, 4b). In terms of aluminum saturation concept (A/CNK molecular ratios), they are predominantly metaluminous to mild peraluminous (0.62- 1.08). Based on Irvine and Baragar's classification (1971), all the analysed rocks plot in the subalkaline and calc-alkaline fields. The content of SiO_2 in these rocks varies from 56.27 to 70.08 wt%.

Figure 4. Classification of the studied volcanic rocks.

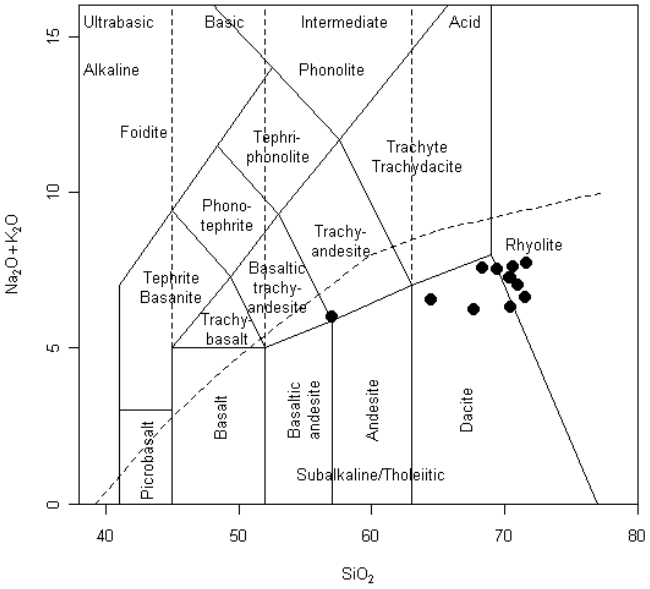

Total alkali-silica diagram (TAS: Le Bas *et al.*, 1986) for the volcanic rocks. Dashed line = subalkaline- alkaline divide (Irvin and Baragar, 1971);

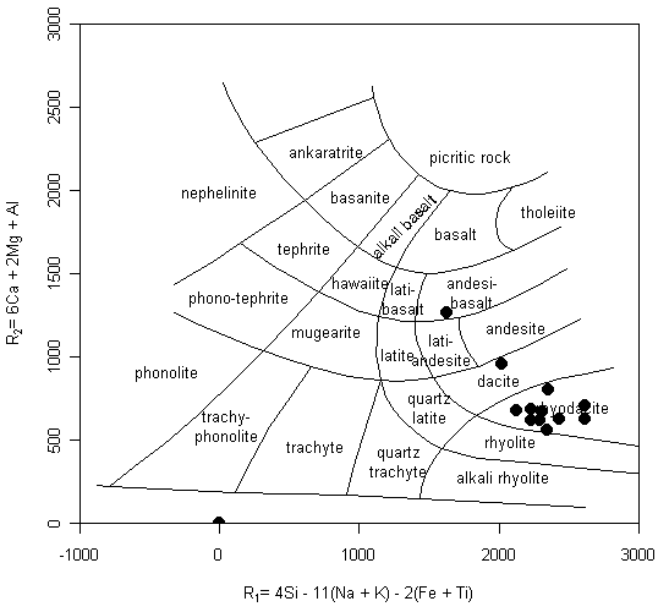

R1-R2 diagram (De La Roche *et al.*, 1980)

Figure 5. Harker variation diagrams

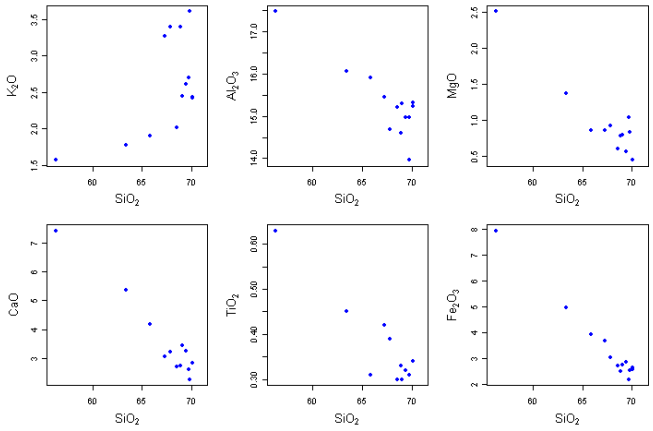

Harker variation diagrams (Major oxides) for the studied volcanic rocks.

In all the samples, the K_2O content increases with increasing SiO_2, whereas the amounts of CaO, Al_2O_3, MgO, TiO_2 and Fe_2O_3 decrease, reflecting the fractional crystallization of hornblende, plagioclase and biotite (Fig.5).

It seems that partial melting of the continental crust led to the formation of dacite parent magma which intruded into shallow-level magma chambers and fractionated. The dacite parent magma mingled with the small volume of mafic magma intruded into magma chamber.

Table 4. Chemical analyses of the Plio-Quaternary volcanic rocks (Central Iran)

	Surk		**Abdollah**	**Buragh**	**Ernan**			**G-Aliabad**		**Ostaj**		**S-Ernan**	**Shamsabad**
Sample	A-10	C-1	Ab-4	Bu-1	Er-4	Re-4	Er-7	Ga-22	Ga-7	Os-1	Os-10	SE-4	Sh-9
SiO_2	67.27	67.81	69.73	65.85	70.08	70.08	69.39	63.4	56.27	69.78	69.87	68.53	69.03
TiO_2	0.42	0.39	0.31	0.31	0.34	0.34	0.32	0.45	0.63	0.31	0.33	0.3	0.3
Al_2O_3	15.46	14.69	14.98	15.91	15.24	15.33	14.97	16.06	17.48	13.96	14.6	15.21	15.3
Fe_2O_3	3.69	3.02	2.18	3.91	2.64	2.57	2.85	4.96	7.95	2.53	2.5	2.7	2.74
MnO	0.04	0.04	0.02	0.07	0.04	0.04	0.03	0.09	0.14	0.04	0.04	0.03	0.02
MgO	0.86	0.93	1.04	0.86	0.45	0.45	0.57	1.37	2.51	0.84	0.79	0.61	0.8
CaO	3.07	3.23	2.6	4.17	2.84	2.84	3.24	5.37	7.42	2.27	2.75	2.71	3.44
Na_2O	4.18	3.97	3.75	4.18	4.48	4.49	4.56	4.64	4.34	3.91	4.04	5.03	3.75
K_2O	3.27	3.39	2.7	1.9	2.44	2.42	2.61	1.78	1.57	3.61	3.39	2.01	2.45

	Surk		**Ab-dollah**	**Bur-agh**	**Ernan**			**G-Alia-bad**		**Ostaj**		**S-Ernan**	**Sham-sabad**
P_2O_5	0.18	0.17	0.11	0.17	0.14	0.13	0.12	0.21	0.36	0.15	0.19	0.1	0.1
LOI	1.3	2.4	2.4	2.1	1.1	1.1	1.1	1.4	1	2.5	2.5	2.7	1.9
Total	99.74	99.82	99.73	99.74	99.79	99.79	99.76	99.73	99.67	99.9	100	99.93	99.83

Discussion

Several petrographical features in the observed plagioclase phenocrysts from the studied rocks such as resorbed appearances, strongly sieve texture, dusty rim or core and the maximum compositional variations from core to rim suggest that these phenocrysts are in disequilibrium, with compositions inconsistent with the current magma.

Moreover, the reverse zoning, the development of reaction rims and the opacite pseudomorph after amphiboles are all features supporting the disequilibrium conditions in dacitic and rhyodacitic amphiboles. On the other hand, some amphiboles are magnesio-hornblende in composition. Magnesio-hornblende in volcanic rocks has been interpreted by some researchers as a result of mixing between basaltic and rhyolitic magma (Heiken and Eichelberger, 1980; Nakada, 1991). The presence of reverse zoning in mafic minerals can be due to increasing P_{H2O} which caused the precipitation of phases with enriched Mg rims in order to reach equilibrium (Sakuyama, 1981; Halsor and Rose, 1991); or more mafic magma invaded the magma chamber (Luhr and Charmichael, 1980; Halsor and Rose, 1991). The reaction textures imply that the magmatic water content for stability of hydrous minerals (such as amphibole and biotite) is too low because of decompression, or introduction and mixing of water-poor melt (Rutherford and Hill, 1993). These mafic mineral features reflect the disequilibrium crystallization with the parent magma.

Based on the geochemistry and mineralogical evidences, it seems that the Plio-Quaternary dacite and rhyodacite from Central Iran formed by melting of continental crust. The disequilibrium textures, mineral compositions and the presence of vesicular magmatic enclaves are all in support of interaction and mingling of dacite and more mafic magma. Following the partial melting of the local continental crust, dacitic magma penetrated the shallow level magma chamber. Amphibole, plagioclase, biotite and quartz crystallized prior to the injection of mafic magma. The presence of reaction rims on the mafic minerals (i.e amphibole, biotite), the sieved textured plagioclase and the rounded and embeyed felsic minerals are due to intrusion of small volume of mafic magma into the magma chamber. The low temperature silicic magma affect on the mafic magma caused quenching of mafic magma and accumulation of some bubbles at the silicic-mafic magma interface. Then mafic magma foamed up and plumes are found. In this entrainment, exchange of xenocrysts (calcic plagioclase and pargasite amphibole) might have occurred and plumes are detached to form the rounded mafic enclaves.

Acknowledgment

This study was supported by the Department of Geology Office of Graduate studies at the University of Isfahan. The authors are grateful to the office for this support.

References

Alavi, M., 1994. Tectonics of the Zagros Orogenic belt of Iran: new data and interpretations. Tectonophysics 220, 211-238. 10.1016/0040-1951(94)90030-2

De La Roche, H., Leterrier, J., Grande Claude, P. and Marchal, M., 1980. A classification of volcanic and plutonic rocks using R1-R2 diagrams and major element analysis, its relationship's and current nomenclature. Chemical Geology 29, 183- 210. 10.1016/0009-2541(80)90020-0

Feeley, T.C., Sharp, Z.D., 1996. Chemical and hydrogen isotope evidence for in situ dehydrogenetion of biotite in silicic magma chambers. Geology 24, 1021–1024. 10.1130/0091-7613(1996)024<1021:CAHIEF>2.3.CO;2

Hajmolaali, A., Alavi, N.M., 1993. Geological map of Khezr-Abad area. Geological Survey of Iran, scale 1:100.000.

Halsor, S.P., Rose, W.I., 1991. Mineralogical relations and magma mixing in calc-alkaline andesites from Lake Atitlan, Guatemala. Mineral. Petrol. 45, 47–67. 10.1007/BF01164502

Heiken, G., Eichelberger, J.C., 1980. Eruptions at Chaos Crags, Lassen Volcanic National Park. J. Volcanol. Geotherm. Res. 7, 443–481. 10.1016/0377-0273(80)90042-6

Irvine, T. N., Baragar, W. R. A., 1971. A guide to chemical classification of common volcanic rocks., Canadian Journal of Earth Sciences. 8, 523-547.

Khalili, M., 1997. Petrography, mineral-chemistry and geochemistry of the Shir-Kuh granite, Southwest of Yadz, Central Iran. Unpublished Ph.D thesis, University of Hamburg, Germany, 143 pp.

Khosrotehrani, K., and Vazirimoghadam, H., 1993. Stratigraphy of Lower Cretaceous in south and southwest of Yazd: Journal of Earth Sciencs, Geological Survey of Iran7, 43-57 (in Persian).

Le Bas M. J., Le Maitre, R. W., Streckeisen A., Zanettin, B., 1986. A chemical classification of volcanic rocks based on the total alkali-silica diagram. J. Petrol. 27, 745-750

Leake, B.E., 1978. Nomenclature of amphiboles. Mineral. Mag. 42, 533–563 10.1180/minmag.1978.042.324.21

Luhr, J.F., Carmichael, I.S.E., 1980. The Colima volcanic complex, Mexico: I. Post-caldera andesites from volcano Colima. Contrib. Mineral. Petrol. 71, 343–372. 10.1007/BF00374707

Nabavi, M. H., 1972, Geological map of Yazd quadrangle, scale 1:250,000: Tehran, Iran, Geological Survey of Iran.

Nakada, S., 1991. Magmatic processes in titanite-bearing dacites, central Andes of Chile and Bolivia. Am. Mineral. 76, 548–560.

Nelson, S. T., Montana, A., 1992. Sieved textured plagioclase in volcanic rocks produced by rapid decompression. Am. Mineral. 77, 1242-1249

Rutherford, M. J., P. M. Hill. 1993. Magma ascent rates from amphibole breakdown: An experimental study applied to the 1980-1986 Mount St. Helens eruption. J. Geophysical Research 98, 19667-19685. 10.1029/93JB01613

Sakuyama, M., 1981. Petrological study of the Myoko and Kurohime Volcanoes, Japan: crystallization sequence and evidence for magma mixing. J. Petrol. 22, 553–583.

Şengör, A.M.C., 1990. A new model for the Late Paleozoic-Mesozoic tectonic evolution of Iran and implication for Oman Region: Geological Society of London. Special Publication 49, 797-831 10.1144/GSL.SP.1992.049.01.49

Shelley, D., 1993. Igneous and metamorphic rocks under the microscope classification, features, microstructure, and mineral preferred orientations, Chapman and Hall, London, 405pp.

Sparks, R.J.S., and Marshall, L.A., 1986. Thermal and mechanical constraints on mixing between mafic and silicic magmas: Journal of Volcanology and Geothermal Research 29, 99-124. 10.1016/0377-0273(86)90041-7

Stamatelopoulou-Seymour, K., Vlassopoulos, D., Pearce, T.H., Rice, C., 1990. The record of magma chamber processes in plagioclase phenocrysts at Thera Volcano, Aegean Volcanic Arc, Greece. Contrib. Mineral. Petrol. 104, 73–84. 10.1007/BF00310647

Stocklin, J., 1968, Structural history and tectonics of Iran: A review. American Association of Petroleum Geologists Bulletin 52, 1229-1258.

Takin, M., 1972. Iranian geology and continental drift in the Middle East. Nature 235, 147-150. 10.1038/235147a0

Tsuchiyama, A., 1985. Dissolution kinetics of plagioclase in melt of the system diopside-albite-anorthite and the origin of dusty plagioclase in andesites. Contrib. Mineral. Petrol. 89, 1-16. 10.1007/BF01177585

Wallace, P.J., Carmichael, I.S.E., 1994. Petrology of Volcan Tequila, Jalisco, Mexico: disequilibrium phenocryst assemblages and evolution of the subvolcanic magma system. Contrib. Mineral. Petrol. 117, 345–361. 10.1007/BF00307270

Zarasvandi, A., Liaghat, S., Zentilli, M., 2004. Evolution of the Darreh-Zerreshk and Ali-Abad porphyry copper deposits, central Iran, within an orogen-parallel strike-slip system [abstract]. In 30th Annual Meeting of Atlantic Geoscience Society, Monckton, New Brunswick, Canada, p.36.

Zarasvandi, A., Liaghat, S., Zentilli, M., 2005. Geology of the Darreh-Zerreshk and Ali-Abad porphyry copper deposits, central Iran. International Geology Review 47, 620-646. 10.2747/0020-6814.47.6.620